
USING DETERMINISTIC TOURIST WALK AS A SMALL-WORLD METRIC ON WATTS-STROGATZ NETWORKS

Joao V. Merenda, Odemir M. Bruno

*Scientific Computing Group
Institute of Physics of Sao Carlos
University of Sao Paulo
joao.merenda@usp.br, bruno@ifsc.usp.br

ABSTRACT

The Watts-Strogatz model (WS) has been demonstrated to effectively describe real-world networks due to its ability to reproduce the small-world properties commonly observed in a variety of systems, including social networks, computer networks, biochemical reactions, and neural networks. As the presence of small-world properties is a prevalent characteristic in many real-world networks, the measurement of "small-worldness" has become a crucial metric in the field of network science, leading to the development of various methods for its assessment over the past two decades. In contrast, the deterministic tourist walk (DTW) method has emerged as a prominent technique for texture analysis and network classification. In this paper, we propose the use of a modified version of the DTW method to classify networks into three categories: regular networks, random networks, and small-world networks. Additionally, we construct a small-world metric, denoted by the coefficient χ , from the DTW method. Results indicate that the proposed method demonstrates excellent performance in the task of network classification, achieving over 90% accuracy. Furthermore, the results obtained using the coefficient χ on real-world networks provide evidence that the proposed method effectively serves as a satisfactory small-world metric.

Keywords Complex networks · Watts-Strogatz model · Small-world networks · Partially self-avoiding walk · Pattern Recognition

1 Introduction

Network science is an interdisciplinary field of research that encompasses various scientific disciplines such as graph theory, statistics, physics, and computer science. Network science has been applied to investigate a wide range of real-world systems, including social networks [1, 2, 3], the spread of diseases [4], metabolic networks [5, 6], neural networks [7], pattern recognition in texture analysis [8, 9], among others. The use of networks and graph theory to study real-world problems dates back to the 18th century, when Leonhard Euler employed graph theory to solve the problem of the seven bridges of Königsberg. Since then, a plethora of network models have been developed.

In 1959, Paul Erdos and Alfred Renyi introduced an algorithm to generate ensembles of random networks. The Erdos-Renyi (ER) model involves adding edges to the graph with a probability p . This can be mathematically represented as $G(N, p)$, where N represents the network size (number of nodes) and p represents the connection probability. Random graphs generated by this model typically exhibit short distances between nodes and a low clustering coefficient. In contrast, regular networks have longer paths between pairs of nodes and a high clustering coefficient. However, many real-world networks, such as neural networks [10] and fictional character networks [1], display the small-world effect, characterized by short diameters, similar to random networks, while also possessing a high clustering coefficient like regular lattices. These networks are referred to as small-world networks [11].

To more accurately model real-world networks, Duncan Watts and Steven Strogatz developed the Watts-Strogatz (WS) model [12]. The WS model begins with a circle network, a regular graph with periodic boundary conditions containing N nodes and degree k . Then, each edge is rewired with a probability p . This process introduces "shortcuts" that connect

two nodes previously separated by a long distance, resulting in a decrease in the average path length. If $p = 0$, no edges are rewired and the network remains regular. If $p = 1$, all edges are rewired to random positions, resulting in a random network. For $0 < p < 1$, shortcuts are created, which quickly decrease the average path length, while only slightly affecting the clustering coefficient. As a result, the process generates a hybrid network that closely mimics many real-world networks.

As many real-world networks possess small-world properties, a metric to quantify this effect, also known as small-worldness, has become crucial. There are various ways to define it, one of the most well-known being the ω (omega) coefficient [13], which is defined as:

$$\omega = \frac{L_{random}}{L} - \frac{C}{C_{lattice}}. \quad (1)$$

This metric compares the clustering coefficient (C) and the average shortest path length (L) of a given network to an equivalent regular network ($C_{lattice}$) and an equivalent random network (L_{random}). This quantity varies from -1 to 1 , and tends to zero when $L \sim L_{random}$, and $C \sim C_{lattice}$, indicating that the network approximates a small-world network.

In the field of pattern recognition, the Deterministic Tourist Walk (DTW) method has been widely used for texture analysis [14, 15, 16] and network classification [17]. The DTW algorithm is an agent-based method, which can be conceptualized as an agent, or "tourist," who visits cities on a map according to deterministic walking rules. In other words, the agent traverses the network by moving from one node to another according to a predefined walking law. The pattern produced by the agent's walk is then used to generate signature vectors for network classification.

In this paper, we propose the use of a modified version of the Deterministic Tourist Walk (DTW) algorithm to investigate the transition between regular and random networks in Watts-Strogatz graphs. Additionally, we utilize the proposed model to construct a new metric for measuring the small-worldness of networks.

2 Deterministic Tourist Walk

The Deterministic Tourist Walk (DTW) is an agent-based method in which an agent, or "tourist," visits nodes according to a predefined walking rule. In the traditional DTW algorithm, which has been applied to texture analysis [14], the agent can move according to two rules: the rule of minimum, in which the agent moves towards the node that minimizes a specific measure (e.g. degree difference between two nodes); and the rule of maximum, in which the agent aims to maximize this measure.

The trajectory of the agent consists of two parts: the transient, which has a length of t , and the attractor, which has a length of a , and occurs when the agent gets stuck in a loop. The total trajectory length is the sum of these two parts. The walker has a memory size (μ) that stores the last μ nodes it has visited. The agent is not allowed to return to a node stored in its memory, resulting in a partially self-avoiding walk. The minimum attractor length is $a = \mu + 1$.

In the proposed method, the agent, or "walker," is launched from every node in the network, resulting in an ensemble of N trajectories, each with a unique value of transient and attractor. Thus, a 2-dimensional histogram illustrating all possible combinations of transient and attractor can be calculated using the following equation:

$$h(\ell) = \sum_{b=1}^{\ell} S(b, \ell - b) \quad (2)$$

where ℓ is the trajectory length and $S(b, \ell - b)$ is a counter function that counts the number of trajectories with transient $t = b$, and attractor size $a = \ell - b$. The $S(t, a)$ function is defined as:

$$S(t, a) = \frac{1}{N} \sum_{i=1}^N \begin{cases} 1, & \text{if } t_i = t, \text{ and } a_i = a \\ 0, & \text{otherwise} \end{cases} \quad (3)$$

In other words, this function calculates the proportion of trajectories with a given transient and attractor size out of the total number of trajectories.

From this histogram, a signature vector $\phi(\mu, r)$, as shown in Eq. 4, is constructed for agents with memory size μ and walking rule r . Traditionally, the first element of the signature vector is the histogram for trajectories with length $\mu + 1$.

$$\phi(\mu, r) = [h(\ell = \mu + 1), h(\ell = \mu + 2), h(\ell = \mu + 3), \dots, h(\ell = N)] \quad (4)$$

Several variations of $\phi(\mu, r)$ have been proposed. In [15], Gonçalves *et al.* proposed concatenating the $\phi(\mu, r)$ vector for multiple memory values to increase the efficiency of the DTW algorithm in classification tasks. This new vector (ψ) is defined by:

$$\psi(\vec{\mu}, r) = \psi([\mu_1, \mu_2, \dots, \mu_m], r) = [\phi(\mu_1, r), \phi(\mu_2, r), \dots, \phi(\mu_m, r)] \quad (5)$$

3 Modified tourist walk

In contrast to the traditional Deterministic Tourist Walk (DTW) method, which is a general approach for any network model, the DTW algorithm presented in this paper includes two modifications to tailor the method for the Watts-Strogatz model. The first modification is in the walking rules, and the second modification is in the construction of the signature vector.

3.1 Walking rules

The first rule is a necessary condition for the agent's movement. The agent moves only if there is a node in its vicinity that has a degree different from the degree of its current node. Mathematically, let k_j be the degree of the j -th neighbor, and k_i be the degree of the current node, then:

$$W_{candidates,i} = \forall j \in W_i : |k_i - k_j| \neq 0 \quad (6)$$

where W_i is the set of neighboring nodes of node i , and $W_{candidates,i}$ is the set of "candidate" neighboring nodes that the agent can choose to visit. The main consequence of this first rule is that if the network is completely regular, *i.e.*, $W_{candidates,i} = \emptyset$ for all nodes in the network, then the agent does not move. In this case, the algorithm returns a transient value (t) of zero and an attractor value (a) of zero. If the first rule is satisfied, *i.e.*, $W_{candidates,i} \neq \emptyset$, the agent moves towards the node that minimizes the difference in the clustering coefficient, as shown in Eq. 7. This is the second walking rule.

$$rule = \min(|c_i - c_j|), \forall j \in W_{candidates,i} \quad (7)$$

where c_i is the clustering coefficient of the current node, and c_j is the clustering coefficient of the j -th candidate node.

There are three stop conditions for the agent's walk: The first one occurs when the agent reaches a locally regular part of the network, and in this case, the algorithm returns a transient value $t = \tau$, and an attractor value $a = 0$, or $t = 0$, and $a = 0$ if the network is entirely regular. The second stop condition occurs when the agent reaches an attractor, and the algorithm returns a transient value $t = \tau$, and an attractor value $a = \alpha$. The last stop condition occurs if the agent does not find an attractor and exceeds the maximum number of iterations allowed (*e.g.*, the network size). In this case, the algorithm returns a transient value $t = N$, and an attractor value $a = 0$.

3.2 The signature vector

In order to adapt the method to these new rules, the term $h(\ell = 0)$ was added to the vector defined by Eq. 4, so the signature vector is now given by

$$\phi(\mu) = [h(\ell = 0), h(\ell = \mu + 1), h(\ell = \mu + 2), \dots, h(\ell = N)] \quad (8)$$

where $h(\ell = 0)$ is a "regularity meter" which is maximum ($h(\ell = 0) = 1$) when the network is completely regular and tends to zero in random networks. The expanded signature vector defined by Eq. 5 remains the same.

3.3 A small-world metric from the DTW algorithm

Let be C the global clustering coefficient of the network $G(V, E)$, and $\bar{\ell}$, the average trajectories length of the tourist walk upon G . Thus, the tourist small-worldness coefficient χ is defined as

$$\chi = C \cdot \frac{\bar{\ell}_G}{\bar{\ell}_{Rand}} \quad (9)$$

where $\bar{\ell}_{Rand}$ is the average length of the trajectories yielded by the tourist in an equivalent random network.

4 Experimental

4.1 Network datasets

In order to test the proposed method was used three datasets.

1. Synthetic-dataset: This synthetic dataset comprises of three network models: i) Random networks, generated using the Erdos-Renyi model, with a probability of connection equal to $p = \langle k \rangle / (N - 1)$; ii) Regular networks, and iii) small-world networks, generated using the Watts-Strogatz model, with $0.01 \leq p \leq 0.1$. The experiments were conducted using four network size values: $N = 500, 1000, 1500, 2000$, and seven average degree values: $\langle k \rangle = 4, 6, 8, 10, 12, 14, 16$. Each of these 28 combinations of N and $\langle k \rangle$ has 100 networks, resulting in 2800 networks for each model and a total of 8400 networks.
2. Noisy-dataset: To evaluate the robustness of the proposed method, noise was introduced to the synthetic-dataset at various rates. Specifically, the experiments were conducted using three noise levels: 10%, 20%, and 30%. The noise was applied by randomly removing or adding edges within the network.
3. Real-world networks: This dataset is composed of networks extracted from the KONECT project [18].

4.2 Classification method

The Linear discriminant analysis (LDA) classifier was employed in the experiment to classify the network datasets. The Leave-one-out cross-validation (LOOCV) approach was used to evaluate the prediction capacity of the model. In the LOOCV method, the dataset is divided into $n - 1$ equal parts, with one data point left out each time. The subset is then classified, and the model returns the average accuracy and the standard deviation.

4.3 Comparison method

A vector Λ containing structural measures of the network was constructed to compare the performance of the proposed method. Four network measures, along with their respective means and standard deviations, were utilized: degree, clustering coefficient, shortest path length, and assortativity. As a result, the vector Λ comprises eight elements.

4.4 Runtime comparison

In the runtime comparison, all experiments were performed using the same computational setup. Intel (R) i7-7820X 32-cores 3.2 GHz, 96 GB RAM, and an Nvidia (R) GTX 1080Ti 11 GB graphic processor unit.

5 Results and discusion

The proposed model results in non-zero trajectories only for networks that do not possess regular properties. Thus, the two-dimensional histogram (transient X attractor) should exhibit a maximum density at the point $(0, 0)$ for regular networks. For random networks, the tourist has a high degree of freedom, and can present trajectories of different sizes in various combinations of transient and attractor lengths. For a rewiring probability of $p = 1.0 \times 10^{-4}$ (as shown in Figure 1(a)), the network is almost regular and exhibits a high density at the point $(0, 0)$. Conversely, for $p = 1.0$ (as shown in Figure 1(f)), there is no trajectory of length zero. In the interval $0.01 \leq p \leq 0.1$ (as shown in Figures 1(c) to 1(e)), a transition occurs, where the network ceases to possess regular properties and becomes increasingly random. However, within this interval, the networks still possess properties of both models, as they are small-world networks.

5.1 Classification

Considering the use of only one memory size μ , Table 1 illustrates that the proposed method demonstrates satisfactory performance in comparison to the structural measures of the network. Utilizing a memory size of $\mu = 1$ yielded the best result, achieving an accuracy of 97% for noise-free networks, and 93%, 87%, 84% for networks with noise rates of $\rho = 10\%, 20\%, 30\%$ respectively. The performance of the DTW method decreases as the memory size increases. The classification of a sample of the dataset containing 300 networks is illustrated in Fig. 2. The addition of noise transforms regular networks into small-world networks and some small-world networks into random networks (Fig 2(b)(c)(d)). As such, it is expected that the method's performance will decrease as noise is added to the network. However, as shown in Table 1, this decrease is not significant and the DTW method maintains an accuracy of over 80% even for networks with 30% noise.

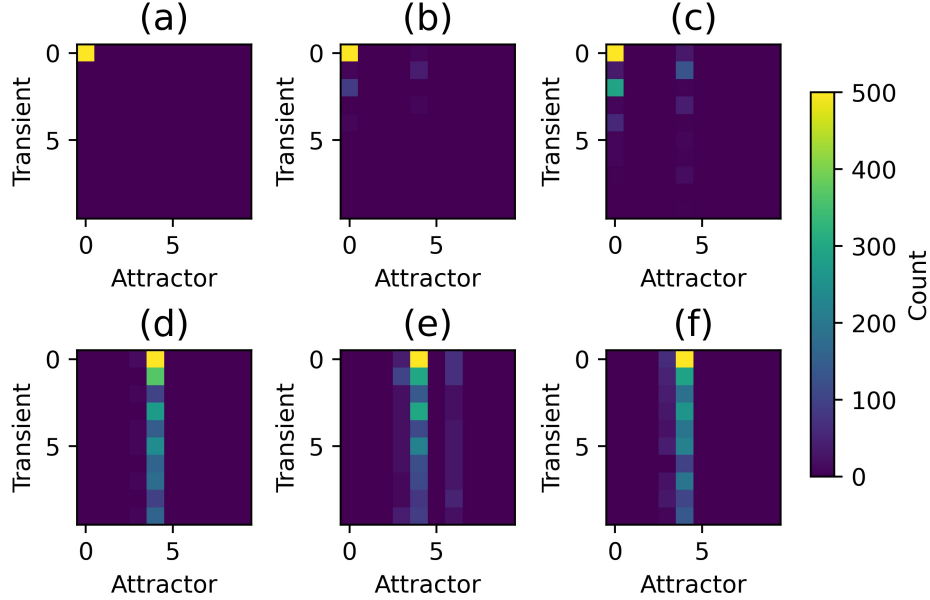


Figure 1: Two-dimensional histogram of the trajectories yielded by the tourist upon a network with 500 nodes and average degree equals 10. The tourist has memory size $\mu = 2$. The outcomes were obtained for some rewiring probabilities p : (a) $p = 0.0001$. (b) $p = 0.001$. (c) $p = 0.01$. (d) $p = 0.05$. (e) $p = 0.1$. (f) $p = 1.0$.

$\phi(\mu)$	synthetic-dataset	Noisy-dataset		
		$\rho = 10\%$	$\rho = 20\%$	$\rho = 30\%$
$\phi(1)$	97 (± 1)	93 (± 3)	87 (± 4)	84 (± 4)
$\phi(2)$	97 (± 1)	92 (± 2)	86 (± 3)	82 (± 3)
$\phi(3)$	97 (± 1)	91 (± 2)	87 (± 3)	83 (± 3)
$\phi(4)$	95 (± 1)	86 (± 3)	84 (± 3)	81 (± 3)
$\phi(5)$	94 (± 1)	85 (± 3)	82 (± 4)	79 (± 4)
Structural measures	98 (± 1)	96 (± 2)	93 (± 2)	91 (± 3)

Table 1: Accuracy (%) and standard deviation for the single-memory tourist approach.

$\psi(\vec{\mu})$	synthetic-dataset	Noisy-dataset		
		$\rho = 10\%$	$\rho = 20\%$	$\rho = 30\%$
$\psi([1, 2])$	99 (± 1)	96 (± 2)	94 (± 2)	90 (± 2)
$\psi([1, 2, 3])$	99 (± 1)	95 (± 2)	97 (± 2)	92 (± 3)
$\psi([1, 2, 3, 4])$	99 (± 1)	99 (± 1)	99 (± 1)	97 (± 1)
$\psi([1, 2, 3, 4, 5])$	100 (± 0)	100 (± 0)	99 (± 1)	99 (± 1)

Table 2: Accuracy (%) and standard deviation for the multiple-memories tourist approach.

When combining multiple memory sizes, the performance of the proposed method improved, as demonstrated in Table 2. Notably, there is a significant gain in accuracy for the noisy dataset. Small memory sizes allow the tourist to extract microscale information from the network, while larger memory values enable the tourist to scan a larger region of the network. By combining several memory values, the deterministic tourist walk method is able to perform a multiscale analysis of the network, thereby extracting more meaningful information about it.

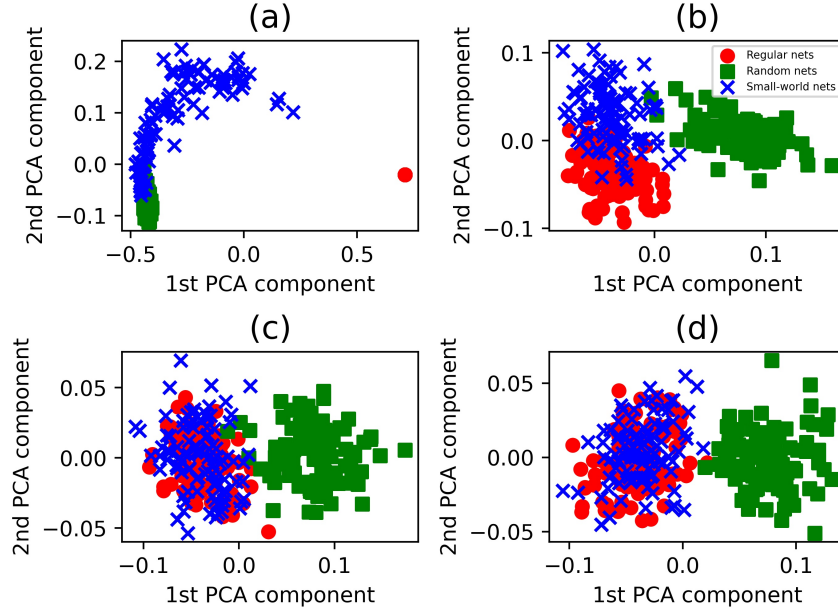


Figure 2: The classification of a sample of the synthetic-dataset by the PCA method. The sample contains 300 networks divided equally into three models: regular networks (in red), random networks (in green), and small-world networks (in blue). (a) Free-noise networks. (b) Networks with 10% of noise. (c) Networks with 20% of noise. (d) Networks with 30% of noise.

5.2 Small-worldness measures

The coefficient χ , defined by Eq. 9, comprises both a structural property of the network, the global clustering coefficient, and a property of the proposed tourist walk method, the trajectory length. As the network becomes more regular or small-world, the global clustering coefficient remains high, while it decreases rapidly as the network becomes more random. In contrast, the average length of the DTW trajectories is zero for regular networks (as the tourist cannot move) and tends to have high values for small-world and random networks (as the tourist has more degree of freedom). Therefore, a peak in the χ curve is expected when both of these measures have high values. Figure 3(c) and (d) show the evolution of these two measures with the rewiring probability. Figure 3(a) and (b) show the coefficient χ (solid lines) and the coefficient ω (dashed lines) within the same range of probability. The coefficient χ presents a peak close to the point where the ω coefficient is zero, indicating that the χ coefficient tends to be the maximum for small-world networks.

As shown in Table 3, the χ values for seven real-world networks are presented. According to the ω coefficient, the Word-adjacency network is more random than the others, thus it is expected that its χ value is low. This network presents the smallest χ coefficients in the table. The *C. elegans* (metabolic) network is more small-world than the *C. elegans* (neural) network. As a result, the first one has a higher χ coefficient than the second one for all memory values.

Network	C	ω	$\gamma_{\mu=1}$	$\gamma_{\mu=2}$	$\gamma_{\mu=3}$	$\gamma_{\mu=4}$
Jazz	0.61	0.009	0.64	0.59	0.44	0.38
Karate club	0.57	0.05	0.59	0.47	0.41	0.45
<i>C. elegans</i> (metabolic)	0.64	0.18	0.56	0.34	0.27	0.32
Football (Girvan-Newman)	0.40	0.32	0.39	0.27	0.28	0.29
<i>C. elegans</i> (neural)	0.29	0.59	0.31	0.15	0.23	0.22
Word adjacency	0.17	0.73	0.16	0.073	0.08	0.13

Table 3: Real-world networks (extracted from [18]) with their respective clustering coefficient (C), ω coefficient, and χ coefficient for memories values: 1, 2, 3, and 4.

In Figure 4, the comparison of the runtime between the χ coefficient and the ω coefficient is shown. With the network size as a constant, and the rewiring probability as a variable, in this first case, the two methods have similar speeds, as

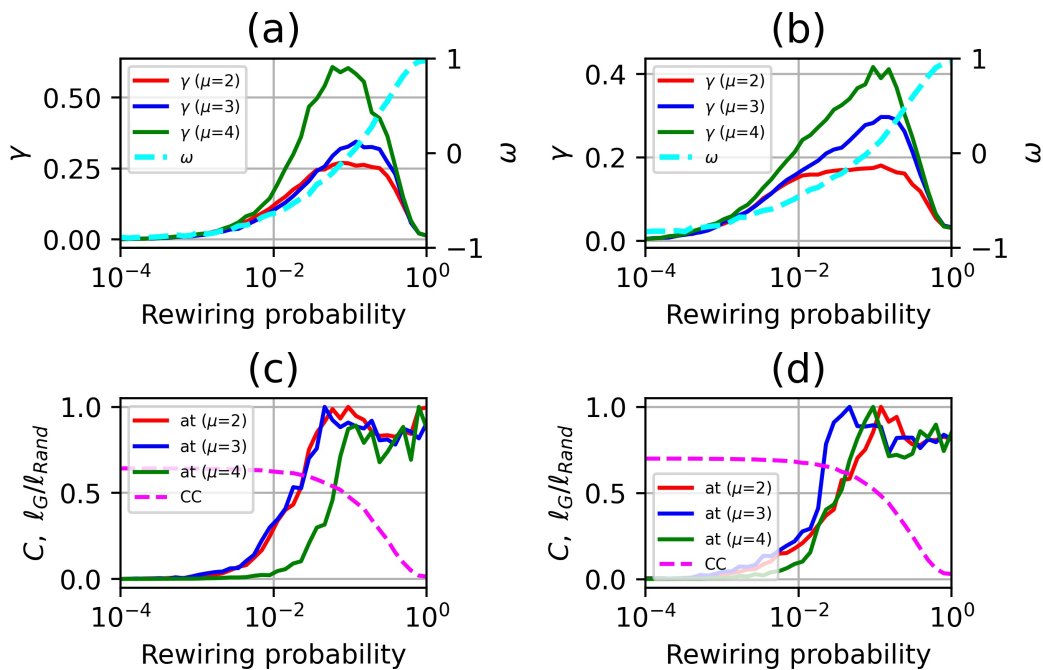


Figure 3: The χ coefficient for Watts-Strogatz networks with rewiring probability ranging from 10^{-4} to 1.0. The red, blue, and green lines represent the DTW method with memory $\mu = 1$, $\mu = 2$, and $\mu = 3$, respectively. The dashed line in magenta represents the clustering coefficient, and the dashed line in cyan represents the ω coefficient. (a) compares the χ coefficient (left axis), and the ω coefficient (right axis) for networks with 500 nodes and average degree $\langle k \rangle = 8$. (b) compares the χ coefficient (left axis), and the ω coefficient (right axis) for networks with 500 nodes and average degree $\langle k \rangle = 16$. (c) compares the clustering coefficient and the average length of the DTW trajectories for networks with 500 nodes and average degree $\langle k \rangle = 8$. (d) compares the clustering coefficient and the average length of the DTW trajectories for networks with 500 nodes and average degree $\langle k \rangle = 16$.

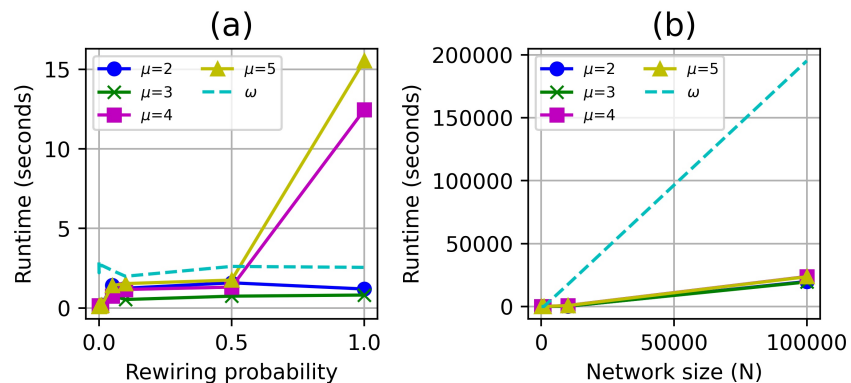


Figure 4: (a) Runtime comparison between χ and ω coefficients for networks with 500 nodes and an average degree equal to 10. The rewiring probability assumes the following values: $p = 0.0001, 0.0005, 0.001, 0.005, 0.01, 0.05, 0.1, 0.5, 1.0$. (b) Runtime comparison for χ and ω , varying the network size: $N = 10^2, 10^3, 10^4, 10^5$. The rewiring probability is $p = 0.05$.

illustrated in Figure 4(a), except for DTW with memory $\mu = 4$ and $\mu = 5$. However, the significant advantage of the proposed method is observed for large networks, as shown in Figure 4(b). As the size of the network increases, the calculation of the χ coefficient proves to be faster than the ω coefficient. All runtime comparisons were performed using the same computational setup.

6 Conclusion

In this paper, a new approach for extracting meaningful information from Watts-Strogatz networks using a partially self-avoiding walk, the deterministic tourist walk, is presented. The novel version of the DTW method introduced here achieved good performance in the classification of networks and highlighted the transition from regular networks to random networks in the WS model. Furthermore, the proposed method also exhibited good results when used as a metric for small-worldness. The small-world effect is prevalent in many real-world networks, making the identification of a metric to quantify this effect crucial. Unlike other metrics that consider only structural properties of the network, the proposed method reached good results by combining a structural property (clustering coefficient) with properties of an automaton (trajectory length). Further studies should be conducted in the future to enhance this method.

Acknowledgements

J.V. Merenda gratefully acknowledges the financial support grant #88887.601525/2021 – 00, Coordination for the Improvement of Higher Education Personnel (CAPES). O. M. Bruno acknowledges support from CNPq (Grant #307897/2018-4) and FAPESP (grants #2018/22214-6 and #2021/08325-2). The authors are also grateful to the NVIDIA GPU Grant Program.

References

- [1] Jiarong Li, Chi Zhang, Huan Tan, and Chunfang Li. Complex networks of characters in fictional novels. In *2019 IEEE/ACIS 18th International Conference on Computer and Information Science (ICIS)*, pages 417–420. IEEE, 2019.
- [2] Stanley Wasserman, Katherine Faust, et al. *Social network analysis: Methods and applications*. Cambridge university press, 1994.
- [3] Robert Axtell. Effects of interaction topology and activation regime in several multi-agent systems. In *International Workshop on Multi-Agent Systems and Agent-Based Simulation*, pages 33–48. Springer, 2000.
- [4] Leonardo FS Scabini, Lucas C Ribas, Mariane B Neiva, Altamir GB Junior, Alex JF Farfán, and Odemir M Bruno. Social interaction layers in complex networks for the dynamical epidemic modeling of covid-19 in brazil. *Physica A: Statistical Mechanics and its Applications*, 564:125498, 2021.
- [5] Jing Zhao, Hong Yu, Jianhua Luo, ZW Cao, and Yixue Li. Complex networks theory for analyzing metabolic networks. *Chinese Science Bulletin*, 51(13):1529–1537, 2006.
- [6] Jeaneth Machicao, Daniel JG Lahr, Marcos Buckeridge, Odemir M Bruno, et al. Topological assessment of metabolic networks reveals evolutionary information. *Scientific reports*, 8(1):1–11, 2018.
- [7] Cornelis J Stam and Jaap C Reijneveld. Graph theoretical analysis of complex networks in the brain. *Nonlinear biomedical physics*, 1(1):1–19, 2007.
- [8] T Chalumeau, L da F Costa, O Lalignant, and F Meriaudeau. Complex networks: application for texture classification. In *Eighth International Conference on Quality Control by Artificial Vision*, volume 6356, page 63561E. International Society for Optics and Photonics, 2007.
- [9] Luciano da Fontoura Costa and Filipi Nascimento Silva. Hierarchical characterization of complex networks. *Journal of Statistical Physics*, 125(4):841–872, 2006.
- [10] Nivedita Chatterjee and Sitabhra Sinha. Understanding the mind of a worm: hierarchical network structure underlying nervous system function in *c. elegans*. In Rahul Banerjee and Bikas K. Chakrabarti, editors, *Models of Brain and Mind*, volume 168 of *Progress in Brain Research*, pages 145–153. Elsevier, 2007.
- [11] L. A. N. Amaral, A. Scala, M. Barthélemy, and H. E. Stanley. Classes of small-world networks. *Proceedings of the National Academy of Sciences*, 97(21):11149–11152, 2000.
- [12] Duncan J Watts and Steven H Strogatz. Collective dynamics of ‘small-world’ networks. *nature*, 393(6684):440–442, 1998.

- [13] Qawi K Telesford, Karen E Joyce, Satoru Hayasaka, Jonathan H Burdette, and Paul J Laurienti. The ubiquity of small-world networks. *Brain connectivity*, 1(5):367–375, 2011.
- [14] André R Backes, Odemir M Bruno, Mônica G Campiteli, and Alexandre S Martinez. Deterministic tourist walks as an image analysis methodology based. In *Iberoamerican Congress on Pattern Recognition*, pages 784–793. Springer, 2006.
- [15] Wesley Nunes Gonçalves, André Ricardo Backes, Alexandre Souto Martinez, and Odemir Martinez Bruno. Texture descriptor based on partially self-avoiding deterministic walker on networks. *Expert Systems with Applications*, 39(15):11818–11829, 2012.
- [16] André Ricardo Backes, Wesley Nunes Gonçalves, Alexandre Souto Martinez, and Odemir Martinez Bruno. Texture analysis and classification using deterministic tourist walk. *Pattern Recognition*, 43(3):685–694, 2010.
- [17] Wesley Nunes Gonçalves, Alexandre Souto Martinez, and Odemir Martinez Bruno. Complex network classification using partially self-avoiding deterministic walks. *Chaos: An Interdisciplinary Journal of Nonlinear Science*, 22(3):033139, 2012.
- [18] J Kunegis. The konect project, 2017.